

# Structure of a New Crystalline Complex: Poly(ethylene oxide) with *p*-Nitrophenol. 1

J. J. Point and P. Damman\*

Service de Chimie Physique-Thermodynamique, Université de Mons Hainaut, Place du Parc, 20, B-7000 Mons, Belgium

Received August 7, 1991; Revised Manuscript Received October 29, 1991

**ABSTRACT:** A new crystalline complex of poly(ethylene oxide) with *p*-nitrophenol is revealed by differential scanning calorimetry, X-ray diffraction, and Fourier transform infrared spectroscopy. The triclinic unit cell ( $a = 1.172$  nm,  $b = 0.555$  nm,  $c = 1.557$  nm,  $\alpha = 90.7^\circ$ ,  $\beta = 87.1^\circ$ , and  $\gamma = 104.0^\circ$ ) is derived from the X-ray fiber patterns of stretched, rolled, and spherulitic samples. The unit cell contains six PEO monomeric units and four *p*-nitrophenol molecules. This composition is derived from the phase diagram and agrees well with the X-ray observations. The phase diagram exhibits the characteristics of a complex eutectic-peritectic system. The molecular complex has the same weight fraction and melting temperature as the second eutectic ( $X_{\text{PNP}} = 0.68$ ,  $T_m = 95^\circ\text{C}$ ). FTIR spectra of the complex show that the vibrations of the PEO chains are greatly affected by the complexation. This observation leads to the conclusion that the chains depart significantly from the 7/2 helical conformation observed for pure PEO. From these data, we suggest that the four *p*-nitrophenol molecules have their benzene rings perpendicular to the chain axis.

## Introduction

Crystalline complexes of poly(ethylene oxide) (PEO) with organic and inorganic compounds such as urea,<sup>1</sup> mercuric halides,<sup>2,3</sup> and *p*-dihalogenobenzene<sup>4</sup> are well-known. In these complexes, the interactions between host and guest molecules differ. In the *p*-dihalogenobenzene complexes, no specific intermolecular forces were found to be present. The complex is formed because the external surface of the macromolecule presents valleys and ridges, the size and shape of which are such that they can accommodate small molecules.<sup>5</sup> The conformation of the polymer molecules is nearly the 10/3 helix,<sup>6</sup> similar to the 7/2 helix observed for the pure PEO. This paper deals with a new crystalline complex formed from a benzenic molecule substituted at the para positions by acceptor and donor groups, *p*-nitrophenol (PNP). Watanabe et al.<sup>7</sup> have shown the potential use of such complexation in nonlinear optic applications. The PNP guest molecules are capable of forming hydrogen bonds; we expect large modifications to the conformation of the PEO chains. By using differential scanning calorimetry, X-ray diffraction, and Fourier transform infrared (FTIR) spectrometry, we prove the existence of such a complex and we elucidate its structure.

## Experimental Section

**Preparation of the Complex.** The PEO-PNP complexes are prepared from PEO of various molecular weights and from *p*-nitrophenol. This is achieved by melting stoichiometric amounts of the two components. High molecular weight ( $M_w = 5000\text{K}$  from Aldrich) is used for stretched and rolled samples, and low molecular weight ( $M_w = 2\text{K}$  or  $6\text{K}$  from Hoechst) is used for spherulitic samples. The homogeneity of the samples is checked by calorimetry.

**Instrumentation and Measurements.** **DSC Measurements.** A Perkin-Elmer DSC4 differential scanning calorimeter is employed for the construction of the phase diagram. The samples are weighed in aluminum sealed capsules. They are first melted and then recrystallized three times to ensure a good homogeneity. The samples are scanned from 0 to  $150^\circ\text{C}$  at a heating rate of  $10^\circ\text{C min}^{-1}$ .

**X-ray Measurements.** Uniaxially oriented specimens are prepared by drawing at room temperature samples quenched from the melt. The doubly oriented specimens are prepared either by rolling at room temperature or by drawing very thin films of the complex prior to crystallization. Other samples are

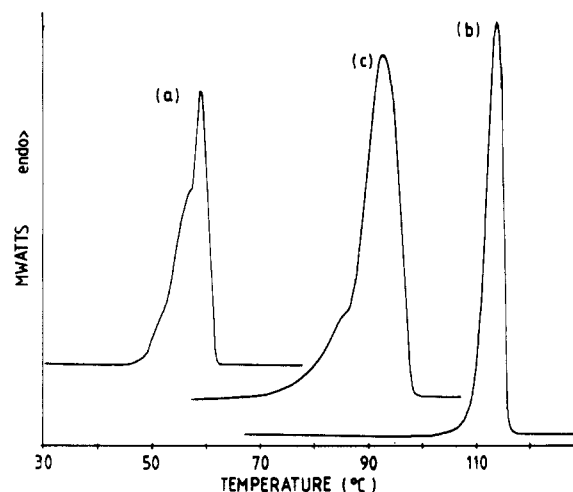


**Figure 1.** DSC traces of pure PEO ( $M_w = 6\text{K}$ ) (a), of pure PNP (b), and of the complex PEO-PNP (c).

obtained by quenching to  $40^\circ\text{C}$  (for PEO,  $M_w = 2\text{K}$ ) or  $50^\circ\text{C}$  (for PEO,  $M_w = 6\text{K}$ ) complex melted at  $135^\circ\text{C}$  in a Lindemann capillary of 1 mm in diameter. The number of nuclei being so low, we managed to obtain X-ray fiber patterns with the capillary, similar to those obtained at the peripheral of a spherulite. X-ray fiber photographs are taken using Ni-filtered  $\text{Cu K}\alpha$  radiation ( $\lambda = 0.15418$  nm) on a Kissig camera with flat plates. In some X-ray photographs, samples were coated with a silver lack used as an internal standard for the estimation of the sample to film distances.

**FTIR Measurements.** The IR spectra are obtained on a Bruker IFS113V Fourier transform infrared spectrometer. Thirty-two coadded interferograms are scanned with a resolution of  $2\text{ cm}^{-1}$ .

**Density Measurement.** The density is determined by flotation in a solution of 1,2-dichloroethane and 1,1,2-trichloroethane, the density of the solution being measured with a pycnometer.

## Results and Discussion

**Preparation of the Complex.** Figure 1 shows the three DSC traces of pure PEO ( $M_w = 6\text{K}$ ), of pure PNP, and of the complex. We can see that the melting peaks of PEO ( $59.1^\circ\text{C}$ ) and PNP ( $113.8^\circ\text{C}$ ) completely disappear in a mixture of the two components with a PNP weight fraction of 0.65. This observation can be explained and interpreted

**Table I**  
**Indexation, Calculated and Observed Spacings, and Coordinates of the Diffraction Spots for a Stretched Sample of the Complex (PEO,  $M_w = 5000K$ ) ( $s_y$  and  $s_z$  Are Reciprocal Distances Respectively Perpendicular and Parallel to the Fiber Axis)**

<i>hkl</i>	$s_{obs}^2/\text{nm}^{-2}$	$s_{calc}^2/\text{nm}^{-2}$	$s_{yobs}/\text{nm}^{-1}$	$s_{zobs}/\text{nm}^{-1}$	$s_{ycalc}/\text{nm}^{-1}$	$s_{zcalc}/\text{nm}^{-1}$
w 100	0.7628	0.7759	0.8714	0.0	0.8788	0.0
m 200	3.1048	3.1037	1.7457	0.0	1.7454	0.0
m 010, 110	3.4919	3.4552, 3.4389	1.8492	0.0	1.8396	0.0
s 110	5.0712	5.0234	2.21774	0.0	2.2076	0.0
m 300	6.9281	6.9833	2.5774	0.0	2.5872	0.0
w 310	12.9773	12.8153	3.4607	0.0	3.4408	0.0
s 011	3.8655	3.8700	1.8406	0.6849	1.8360	0.6432
m 1,1,-1	5.4991	4.4936	2.1974	0.6720	2.2137	0.6432
w 3,-1,1	8.2467	8.3103	2.7519	0.6880	2.7361	0.6432
w 3,-1,-1	8.5754	8.6429	2.7803	0.6850	2.7902	0.6432
w 311	13.1996	13.0638	3.4196	0.6809	3.4111	0.6432
w 002	1.6656	1.6592	0.0	1.2842		
m 102	2.3111	2.3242	0.8291	1.2916	0.7982	1.2865
w 202	4.5202	4.5411	1.6558	1.2737	1.6624	1.2865
m 012	5.0712	5.1144	1.8130	1.2817	1.8177	1.2865
s 2,-1,-2	6.8115	6.8554	2.1854	1.2865	2.2184	1.2865
m 302	8.2058	8.3099	2.4942	1.2975	2.4989	1.2865
s 2,1,-2	9.9625	10.0243	2.7609	1.3448	2.7879	1.2865
s 1,-1,3	7.3208	7.3384	1.7614	1.9662	1.7293	1.9297
w 2,-1,3	8.4518	8.3750	2.0987	1.8969	2.0578	1.9297
w 1,1,-3	8.8241	8.9229	2.1526	1.8876	2.1739	1.9297
w 3,-1,3	11.3457	11.2961	2.6395	1.9020	2.6104	1.9297
w 313	16.6436	16.0495	3.3472	1.6916	3.2856	1.9297
w 3,1,-3	17.5366	17.0473	3.4449	2.0243	3.4054	1.9297
m 004	6.5802	6.6367	0.0	2.5145		
s 104	7.1629	7.1909	0.5747	2.5695	0.5136	2.5729
s 014	10.0479	10.0920	1.6989	2.6076	1.6932	2.5729
w 3,1,-4	19.9687	20.1172	3.2849	2.6006	3.3305	2.5729
w 314	18.2928	18.7868	3.1600	2.5631	3.1732	2.5729

**Table II**  
**Indexation, Calculated and Observed Spacings, and Coordinates of the Diffraction Spots for Spherulitic Fibers of the Complex (PEO,  $M_w = 2K$ ) ( $s_y$  and  $s_z$  Are Reciprocal Distances Respectively Perpendicular and Parallel to the Fiber Axis)**

<i>hkl</i> <sup>a</sup>	$s_{obs}^2/\text{nm}^{-2}$	$s_{calc}^2/\text{nm}^{-2}$	$s_{yobs}/\text{nm}^{-1}$	$s_{zobs}/\text{nm}^{-1}$	$s_{ycalc}/\text{nm}^{-1}$	$s_{zcalc}/\text{nm}^{-1}$
m 004	6.4006	6.6367	2.418	0.0	2.5217	0.1259
m 014	9.8754	10.0920	3.04912	0.0	3.0630	0.3238
m 100	0.7683	0.7759	0.0	0.8746		
w 102*	2.3497	2.3242	1.2916	0.8303	1.2740	0.8179
w 010	3.4825	3.4552	1.7650	0.5004	1.7838	0.4497
s 011	3.8440	3.8700	1.8748	0.4981	1.8990	0.4182
w 012	5.0088	5.1144	2.1868	0.4463	2.1930	0.3868
m 013	7.0952	7.1884	2.5463	0.6083	2.5991	0.3553
s 200	3.1356	3.1037	0.0	1.7543		
w 202	4.5720	4.5411	1.2116	1.7850	1.2380	1.6988
m 110	5.008	5.0234	1.7584	1.3924	1.7616	1.3306
m 1,1,-1	5.4980	5.4936	1.8805	1.3749	1.8599	1.3620
m 1,1,-2	6.8065	6.7934	2.1371	1.4393	2.1395	1.3935
s 300	6.9710	6.9833	0.0	2.5852		
w 210*	8.2829	8.1434	1.0268	2.5669	1.6908	2.2114
m 211*	8.4566	8.4473	1.7927	2.2196	1.8086	2.1800
m 3,-1,-2	10.0108	10.0536	2.0485	2.2325	2.0891	2.2558

<sup>a</sup> Asterisks indicate broad diffractions.

by the existence of a molecular complex. The existence of a definite molecular complex is documented hereafter on the basis of X-ray diffraction, FTIR, and calorimetric data.

**X-ray Analysis. Unit Cell.** Parts a and b of Figure 2 show the X-ray fiber patterns of a stretched sample and of a spherulite of the new compound, respectively. These diagrams do not show any reflections characteristic of the pure PEO or of the pure PNP. We have therefore a direct proof of the existence of a new crystalline phase formed from PEO and PNP. To determine the unit cell of this molecular complex, we first examined the stretched sample. The (002) and (004) reflections along the fiber axis give the value of reciprocal axis  $c^*$ . Second, the indexation of the equatorial reflections, which have Miller indices of the form ( $h$  $k$ 0), leads to the reciprocal parameters  $a^*$ ,  $b^*$ , and  $\gamma^*$ . Finally, we calculate the positions of the diffraction spots on the X-ray photograph which give

the reciprocal angles  $\alpha^*$  and  $\beta^*$  equal to  $90^\circ$  and  $92.8^\circ$ , respectively. The proposed unit cell has the following parameters:  $a = 1.172$  nm,  $b = 0.555$  nm,  $c = 1.557$  nm,  $\alpha = 90.7^\circ$ ,  $\beta = 87.1^\circ$ , and  $\gamma = 104.0^\circ$ . This agrees with all the observed reflections for the stretched and spherulitic samples which have different fiber axes  $c$  and  $a^*$  respectively. Tables I and II show the indexation, the calculated and observed spacings, and coordinates of the diffraction spots for the two samples. The disposition of the PNP molecules may be determined from the X-ray photographs. In fact, only the (004) reflection is intense along the fiber axis of the drawn sample, and the value of  $c/4 = 0.389$  nm agrees well with the distance between the benzene rings observed in pure PNP,  $\beta$  modification.<sup>8</sup> From these observations, we can suggest that four PNP molecules are stacked along the  $c$  crystallographic parameter (the chain axis). This interpretation is corroborated by measurement of IR dichroism (to be published). Table III shows the

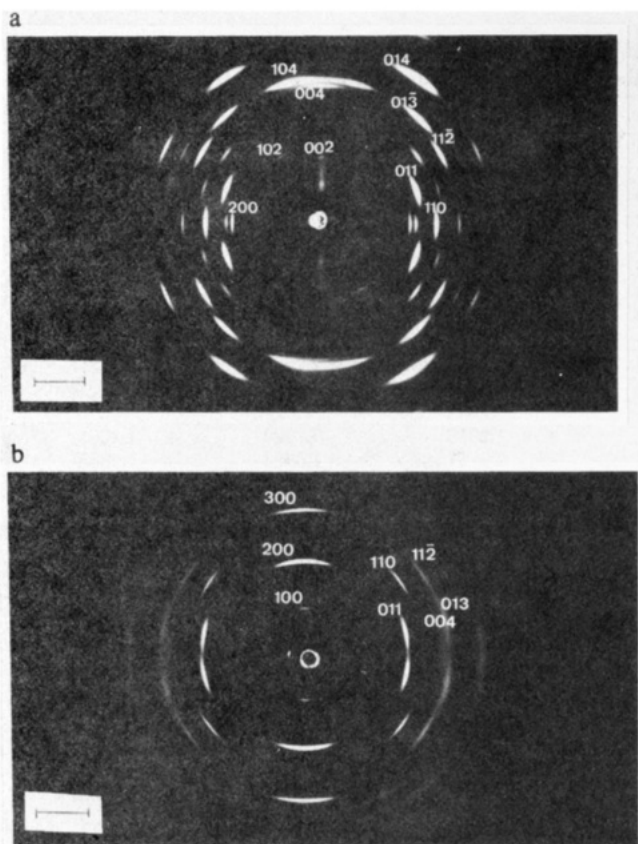


**Figure 2.** X-ray fiber diagrams of stretched fibers (a) and of spherulitic fibers (b) of the complex PEO-PNP. The fiber axis is vertical. The scale bar corresponds to  $1 \text{ nm}^{-1}$  with  $\lambda = 0.15418 \text{ nm}$ .

**Table III**  
Calculated Density and Stoichiometry as a Function of the Number of Monomeric Units of PEO for the Complex

no. of monomeric units of PEO	density, $\text{g/cm}^3$	stoichiometry (PNP weight fraction)
4	1.242	0.760
5	1.317	0.716
6	1.392	0.678
7	1.467	0.644
8	1.541	0.612

density and stoichiometry as a function of the possible number of monomeric units of PEO. From the experimental density of  $1.34 \text{ g/cm}^3$  and the approximate stoichiometry (PNP weight fraction of 0.65), we deduce that the unit cell contains six monomeric units and four PNP molecules.

**Doubly Oriented Samples.** We obtained doubly oriented samples by stretching amorphous films of the complex PEO-PNP. Parts a-c of Figure 3 show X-ray photographs of the stretched film and the indexation of their most intense observed reflections for the three orientations N, E, and T. All reflections are indexed with the triclinic unit cell. We can explain this double orientation on the basis of the anisotropy of the transversal contraction which occurs during the stretching of a thin polymeric film. The study on the rolled sample of the complex confirms this hypothesis. In fact, the X-ray photographs obtained for the three orientations N, L, and T are the same as for the doubly oriented stretched samples (see Figure 4a-c). The  $c$  crystallographic axis is oriented along the rolling or the stretching direction, and the  $a^*$  reciprocal axis is oriented in the plane of the samples.

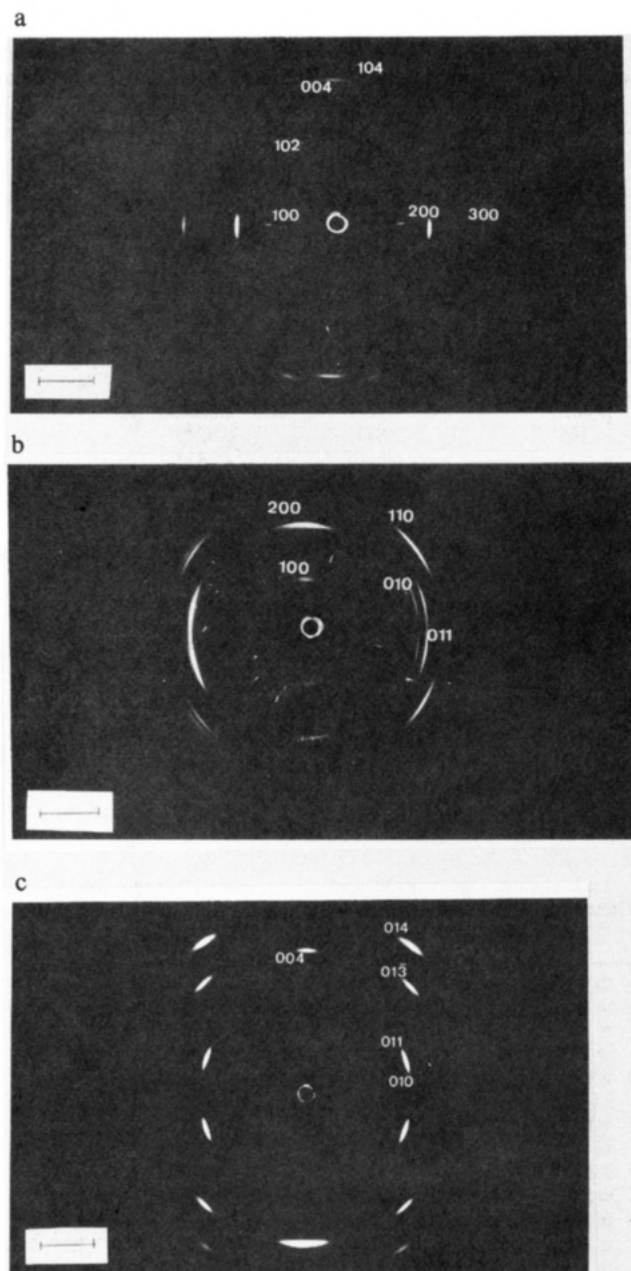


**Figure 3.** X-ray fiber diagrams of a doubly oriented stretched sample of complex with orientations (a) N, (b) E, (c) T. The scale bar corresponds to  $1 \text{ nm}^{-1}$  with  $\lambda = 0.15418 \text{ nm}$ .

**Phase Diagram.** The phase diagram of the oligomeric PEO ( $M_w = 6\text{K}$ ) and PNP gives supplementary proof to the formation of a complex (Figure 5). In fact, it shows a bell-shape region, characteristic of the molecular complex, separated by two eutectics. The PNP weight fraction and melting temperature are respectively 0.25 and  $42^\circ\text{C}$  for the first eutectic and 0.68 and  $95^\circ\text{C}$  for the second eutectic. The phase diagram has the characteristics of a eutectic-peritectic system, similar to the PEO-hydroquinone molecular complex.<sup>9</sup> The PEO-PNP complex has the same weight fraction and melting temperature as the second eutectic. The stoichiometry corresponds to a PNP weight fraction of 0.68 and agrees with our proposal of four molecules of PNP and six monomeric units of PEO which gives a theoretical value of 0.678 for the stoichiometry.

**FTIR Analysis.** Figure 6 shows the FTIR spectra obtained for PEO and the complex. The IR bands of the PNP are weakly affected by the complexation, except for the bands characteristic of hydrogen bonds. The frequency

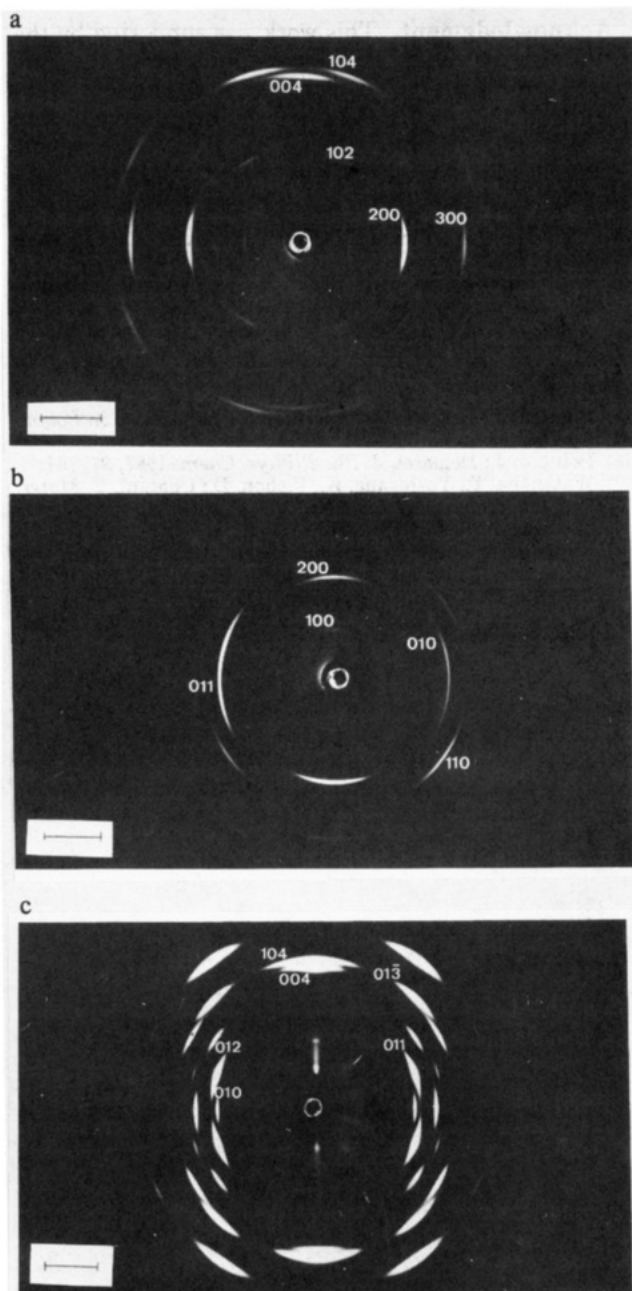


**Figure 4.** X-ray diagrams of a rolled sample of complex with orientations (a) N, (b) L, and (c) T. The scale bar corresponds to  $1 \text{ nm}^{-1}$  with  $\lambda = 0.15418 \text{ nm}$ .

of the OH stretching is  $3325 \text{ cm}^{-1}$  in the crystalline PNP and  $3271 \text{ cm}^{-1}$  in the complex. However, the IR bands of the polymer are greatly affected by the complexation (Table IV). The bands observed for the pure PEO 7/2 helical conformation<sup>10</sup> completely disappear, and we observe new IR bands characteristic of the PEO in the complex. This suggests that the conformation of the polymer chains departs significantly from that of pure PEO. This is not unusual for complexes in which the interactions between host and guest molecules are strong.<sup>2,3</sup> The number of observed vibrations for the polymer in the complex is lower than that for the pure PEO. This suggests that the symmetry of the PEO chain in the complex is higher than that in pure polymer. Similar observations have been made with regard to the IR spectra of planar PEO zigzag chains.<sup>11</sup> Various possible conformations may account for the observed value of  $c = 1.557 \text{ nm}$ . The determination of the exact conformation is still in progress.

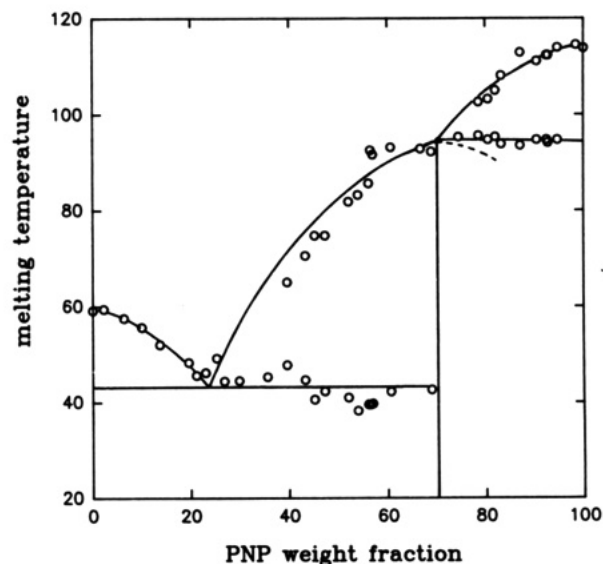


**Figure 5.** Phase diagram of PEO ( $M_w = 6K$ ) and PNP.

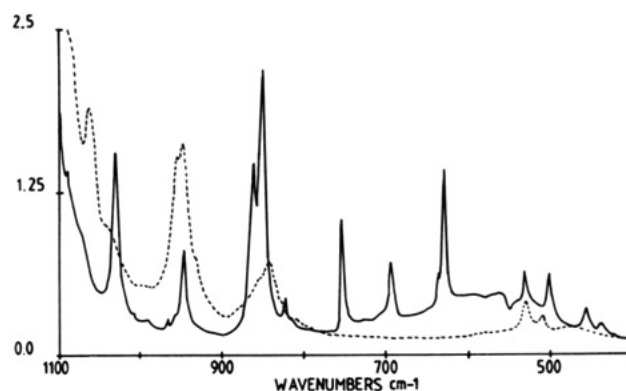


**Figure 6.** FTIR spectra of isotropic films of PEO (broken line) and of the complex PEO-PNP (solid line).

**Table IV**  
Observed Wavenumbers for Pure PEO and for the PEO in the Complex

obs wavenumbers of pure PEO/ $\text{cm}^{-1}$	obs wavenumbers of PEO in the complex/ $\text{cm}^{-1}$
m 107	m 121
w 163	m 158
w 216	w 207
	w 237
	m 455
w 509	
w 529	
w 532	
s 841	m 871
m 945	m 947
s 959	
s 1061	s 1032
s 1147	s 1135
s 1240	w 1231
s 1279	s 1248
s 1340	
m 1358	m 1385
w 1413	
m 1453	m 1458
w 1462	
s 1467	
s 2859	sh 2877
s 2885	s 2892
w 2945	sh 2932
	s 2930

## Conclusions

From X-ray diffraction and differential scanning calorimetry, the existence of a new crystalline complex formed

from PEO and PNP has been demonstrated. A triclinic unit cell ( $a = 1.172$  nm,  $b = 0.555$  nm,  $c = 1.557$  nm,  $\alpha = 90.7^\circ$ ,  $\beta = 87.1^\circ$ , and  $\gamma = 104.0^\circ$ ) has been determined from fiber patterns of the different studied samples (stretched, rolled, or spherulitic). The unit cell consists of six PEO monomeric units and four PNP molecules. The phase diagram exhibits the characteristics of a eutectic-peritectic system. The complex has the same weight fraction and melting temperature as the second eutectic ( $x_{\text{PNP}} = 0.68$ ,  $T_m = 95^\circ\text{C}$ ). FTIR spectra of PEO and of the complex show that the vibrations of the PEO chains are greatly affected by the complexation. This observation leads to the conclusion that the chains depart significantly from the 7/2 helical conformation of pure PEO. From the X-ray observations, we suggest that the four PNP molecules have their benzene rings nearly perpendicular to the chain axis ( $c$  crystallographic parameter). A detailed infrared study of the complex is still actively in progress, which should provide an insight into the exact conformation adopted by the PEO chains and the orientation of the PNP molecules with respect to the unit cell.

**Acknowledgment.** This work was supported by the "Ministère de la Région Wallonne, programme de Formation et d'Impulsion à la Recherche Scientifique et Technologique" and by the FNRS (Fonds de la Recherche Scientifique, Belgium).

## References and Notes

- (1) Tadokoro, I.; Yoshihara, T.; Chatani, Y.; Murahashi, S. *Polym. Lett.* **1964**, *2*, 369.
- (2) Iwamoto, R.; Saito, Y.; Ishihara, H.; Tadokoro, H. *J. Polym. Sci., Polym. Phys. Ed.* **1968**, *6*, 1509.
- (3) Yokoyama, M.; Ishihara, H.; Iwamoto, R.; Tadokoro, H. *Macromolecules* **1969**, *2*, 184.
- (4) Point, J. J.; Coutelier, C. *J. Polym. Sci., Polym. Phys. Ed.* **1985**, *23*, 231.
- (5) Point, J. J.; Damman, P., accepted for publication in *Polym. Commun.*
- (6) Point, J. J.; Demaret, J. Ph. *J. Phys. Chem.* **1987**, *91*, 797.
- (7) Watanabe, T.; Yoshigana, K.; Fichou, D.; Chatani, Y. *Mater. Res. Soc. Proc.* **1988**, *109*, 339.
- (8) Coppens, P.; Schmidt, G. H. *J. Acta Crystallogr.* **1965**, *18*, 654.
- (9) Myasnikova, R. M. *Vysokomol. Soedin.* **1976**, *A19*, 564.
- (10) Yoshihara, T.; Tadokoro, H.; Murahashi, S. *J. Chem. Phys.* **1964**, *41*, 2902.
- (11) Ramana Rao, G.; Castiglioni, C.; Gussoni, M.; Zerbi, G.; Martuscelli, E. *Polymer* **1985**, *26*, 811.